Acta Pharmaceutica Sinica B 2020;10(9):1754−1768

Chinese Pharmaceutical Association
Institute of Materia Medica, Chinese Academy of Medical Sciences

Acta Pharmaceutica Sinica B

www.elsevier.com/locate/apsb
www.sciencedirect.com

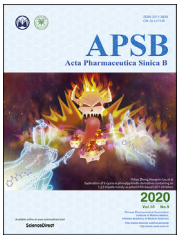

ORIGINAL ARTICLE

Inhibition of post-trabeculectomy fibrosis *via* topically instilled antisense oligonucleotide complexes co-loaded with fluorouracil

Kuan Jiang[a,†], Junyi Chen[b,†], Lingyu Tai[a,c,†], Chang Liu[a], Xishan Chen[a], Gang Wei[a,d,e,*], Weiyue Lu[a,d], Weisan Pan[c,*]

[a]*Key Laboratory of Smart Drug Delivery, Ministry of Education; Department of Pharmaceutics, School of Pharmacy, Fudan University, Shanghai 201203, China*
[b]*Department of Ophthalmology, Eye & ENT Hospital, Fudan University, Shanghai 200031, China*
[c]*School of Pharmacy, Shenyang Pharmaceutical University, Shenyang 110016, China*
[d]*The Institutes of Integrative Medicine of Fudan University, Shanghai 200040, China*
[e]*Shanghai Engineering Research Center of Immunotherapeutics, Shanghai 201203, China*

Received 30 December 2019; received in revised form 17 February 2020; accepted 27 February 2020

KEY WORDS

Trabeculectomy;
Fibrosis prevention;
Gene delivery;
Penetratin;
Fluorouracil

Abstract Trabeculectomy is the mainstay of surgical glaucoma treatment, while the success rate was unsatisfying due to postoperative scarring of the filtering blebs. Clinical countermeasures for scar prevention are intraoperative intervention or repeated subconjunctival injections. Herein, we designed a co-delivery system capable of transporting fluorouracil and anti-TGF-β2 oligonucleotide to synergistically inhibit fibroblast proliferation *via* topical instillation. This co-delivery system was built based on a cationic dendrimer core (PAMAM), which encapsulated fluorouracil within hydrophobic cavity and condensed oligonucleotide with surface amino groups, and was further modified with hyaluronic acid and cell-penetrating peptide penetratin. The co-delivery system was self-assembled into nanoscale complexes with increased cellular uptake and enabled efficient inhibition on proliferation of fibroblast cells.

Abbreviations: ASO, antisense oligonucleotide; DAPI, 4′,6-diamidino-2-phenylindole; DLS, dynamic light scattering; EE, encapsulation efficiency; EGF, epidermal growth factor; FAM, 6-carboxyfluorescein; FBS, fetal bovine serum; FITC, fluorescein 5-isothiocyanate; Fu, fluorouracil; GAPDH, glyceraldehyde-3-phosphate dehydrogenase; HA, hyaluronic acid; HRP, horseradish peroxidase; IBAGS, the Indiana Bleb Appearance Grading Scale; IOP, intraocular pressure; L929, murine fibroblast cells; MWCO, molecular weight cut-off; PAGE, polyacrylamide gel electrophoresis; PAMAM, poly(amidoamine); PEI, polyethylenimine; Pene, penetratin; PG5, PAMAM G5−NH_2; PLGA, poly(lactic-*co*-glycolic acid); PVDF, polyvinylidene difluoride; SDHCEC, human corneal epithelial cells; SDS, sodium dodecyl sulfate; TEM, transmission electron microscope; TGF-β, transforming growth factor-β.

*Corresponding authors. Tel.: +86 21 51980091, fax: +86 21 51980090 (Gang Wei); Tel.: +86 24 23986313, fax: +86 24 23953241 (Weisan Pan).
E-mail addresses: weigang@shmu.edu.cn (Gang Wei), ppwwss@163.com (Weisan Pan).
[†]These authors made equal contributions to this work.
Peer review under responsibility of Chinese Pharmaceutical Association and Institute of Materia Medica, Chinese Academy of Medical Sciences.

https://doi.org/10.1016/j.apsb.2020.03.002

In vivo studies on rabbit trabeculectomy models further confirmed the anti-fibrosis efficiency of the complexes, which prolonged survival time of filtering blebs and maintained their height and extent during wound healing process, exhibiting an equivalent effect on scar prevention compared to intraoperative infiltration with fluorouracil. Qualitative observation by immunohistochemistry staining and quantitative analysis by Western blotting both suggested that TGF-β2 expression was inhibited by the co-delivery complexes. Our study provided a potential approach promising to guarantee success rate of trabeculectomy and prolong survival time of filtering blebs.

1. Introduction

Glaucoma is a frequently occurring ophthalmic disease and the overt symptom is elevated intraocular pressure (IOP), which leads to a series of optic neuropathy and potentially irreversible vision loss[1]. Over 60 million individuals are affected with glaucoma worldwide in 2010 and the number of cases is expected to reach 80 million till 2020[2]. According to clinical studies, decreasing IOP to a normal level has been demonstrated to be an efficient method to alleviate the progression of glaucoma. Surgery is one of the main treatments to lower IOP in clinic, among which trabeculectomy is the most commonly applied procedure. However, the complete success rate of trabeculectomy is only around 40%, while over half of surgical effects are influenced by postoperative scarring[3,4].

In general, the aim of trabeculectomy is to create an additional transscleral route towards the subconjunctival space by trabecula resection. This artificial passage can achieve aqueous drainage so that the extra aqueous humor would elevate the subconjunctival area resulting in forming a filtering bleb. At last, aqueous drainage will be absorbed by the conjunctival vasculature after passing the filtering bleb. Nevertheless, during postsurgical wound healing progress, there is a high propensity of subconjunctival fibrous tissue formation, which may block the filtering passage with proliferous cicatricial tissue. Extensive studies have been carried out to prevent fibroblasts proliferation and to increase the success rate of trabeculectomy[5].

For fibrosis prevention in filtering glaucoma surgery, current strategy mainly focuses on inhibition of fibroblast cells proliferation. For inhibition of inflammation and proliferation, cytotoxic antimetabolites such as fluorouracil (Fu) and mitomycin C are the mainstay of clinical anti-scarring interventions[6]. However, they are mainly used *via* local injection or intraoperative infiltration considering the risk of their side-effects. Recent studies have explored the feasibility to deliver small molecule drugs to the eye through topical administration route using poly(amidoamine) (PAMAM) as a carrier. Complexation could be formed between dexamethasone and PAMAM, resulting in increased transportation across both cornea and sclera tissues[7]. Additionally, the PAMAM complex was verified to improve the bioavailability of puerarin and prolonged its half-life in aqueous humor of rabbits after topical administration[8]. It was reported that fluorouracil was also able to form supramolecular complexes with PAMAM in aqueous solution, which may be employed to improve fluorouracil delivery[9]. These findings have prompted a possible way for sustained ocular delivery of fluorouracil *via* noninvasive administration utilizing PAMAM dendrimer.

Inhibition of related growth factors after filtering surgery is another strategy for fibrosis prevention[10]. Studies conducted to inhibit growth factors mainly focused on the myofibroblast transdifferentiation-related transforming growth factor-β (TGF-β). It has been reported that the TGF-β2 isoform played a predominant role in scarring responses after glaucoma filtration surgery, and inhibition on TGF-β2 could improve the success rate[11]. Among all the biological modulators, antisense oligonucleotides (ASOs) have been extensively studied because of their gene-silencing effects at low dose and synergetic function in clinical therapy. ASOs are often applied in a condensation form with cationic polymers such as PAMAM dendrimers and polyethylenimine (PEI). Previous studies have shown that ASO/PEI complex (specific targeting TGF-β2) encapsulated in poly(lactic-*co*-glycolic acid) (PLGA) microspheres could improve bleb survival in a rabbit filtering surgery model after subconjunctival injection[12]. However, biological modulators possess poor permeability in ocular absorption barrier and are usually difficult to be endocytosed by the cells even being administrated as implants or by injections[13].

Both chemical drugs and biological modulators show promising potential in fibrosis prevention; however, their applications are limited by administration routes. Intraoperative interventions cannot achieve a sustained prevention effect, while repeated injections or subconjunctival implants may trigger inflammation and hence reduce patient compliance[14]. Based on clinical studies, it is suggested that fibrosis prevention would benefit more from frequent applications other than intermittent applications[15]. In consideration of the above concern, a topical formulation, which can effectively deliver anti-fibrosis drugs to surgical site *via* a noninvasive way, is required urgently.

In this work, we proposed to develop a co-delivery system combining gene therapy with chemotherapy in order to prevent the formation of postoperative scar in filtering blebs. ASO and fluorouracil were chosen to implement a synergistic inhibition on the proliferation of fibrous cells, and the synergistic effect of the co-delivery system would be assessed. Moreover, this co-delivery system aimed to improve ocular absorption *via* topical instillation. We applied PAMAM G5−NH_2 (PG5) as a carrier core to condense ASO, which was specific for TGF-β2, as well as to encapsulate fluorouracil (Dual/PG5 complex). The dual drug-loading was achieved by incorporating fluorouracil in the hydrophobic cavity of PG5 dendrimer and condensing ASO with amino groups on the surface of dendrimer. In this case, the ocular permeability of PG5 would be impaired since the functional groups on PG5 were partially occupied by ASO and fluorouracil. Cell-penetrating peptides have been widely reported as potential tools to

overcome various physiological barriers[16]. Penetratin is a cell-penetrating peptide derived from a non-virus originated protein. In our previous work, penetratin was screened out as an ocular permeation enhancer for its quick intraocular distribution and low tissue toxicity[17]. Considering PG5 and penetratin were both electropositive, low molecular weight hyaluronic acid (HA) was introduced as an electronegative linker between PG5 and penetratin (Dual/PG5/HA complex). Finally, penetratin was non-covalently modified on the outer surface of Dual/PG5/HA complex (Dual/PG5/HA/Pene complex). All the complexation during preparation of the delivery system was assembled by electrostatic interaction and was easy to process.

Accordingly, we prepared a series of complexes for *in vitro* and *in vivo* evaluation of their anti-fibrosis effects. *In vivo* trabeculectomy model was established with rabbits and the complexes were evaluated for their ability to prolong the survival of filtering blebs *via* topical instillation. The aim of this study is to explore the noninvasive delivery approach for prevention of postoperative fibrosis proliferation after trabeculectomy. This alternative treatment with antisense oligonucleotide and fluorouracil was expected to effectively inhibit bleb area from scarring at low administration dose without injuring normal ocular tissues, which may be of great potential to increase the success rate of trabeculectomy and to relieve post-surgery suffering.

2. Materials and methods

2.1. Materials

PAMAM G5−NH_2 (PG5) was purchased from Sigma−Aldrich (St. Louis, MO, USA), and labeled with fluorescein isothiocyanate (Sigma−Aldrich) in our laboratory (PG5-FITC). Antisense oligonucleotide (ASO) targeting TGF-β2 with a sequence of 5′-CCGTGACCAGATGCAGGAT-3′ was synthesized by Sangon Biotech (Shanghai, China). ASO labeled with 6-carboxyfluorescein (FAM) at 5′-end was assigned as ASO-FAM. Hyaluronic acid sodium salt (HA, 6 kD) was purchased from Freda Biochem (Jinan, China). Penetratin (Pene, RQIKIWFQNRRMKWKK) was provided by ChinaPeptides Co., Ltd., (Shanghai, China). Fluorouracil was purchased from Yuanye Co., Ltd., (Shanghai, China). All other biochemical reagents used in this work were purchased from Sigma−Aldrich and all the chemicals used in this work were of analytical grade.

Murine fibroblast cells (L929) were kindly provided by Stem Cell Bank, Chinese Academy of Sciences (Shanghai, China) and cultured at 37 °C in a 5% CO_2 humidified atmosphere and DMEM medium supplemented with 4 mmol/L glutamine. Human corneal epithelial cells (SDHCEC) were kindly donated by Zhongshan Ophthalmic Center, Sun Yat-sen University (Guangzhou, China) and cultured in DMEM medium supplemented with 5 mg/mL insulin, 10 ng/mL human EGF and 1% (*w*/*v*) hydrocortisone. All medium was supplemented with 10% fetal bovine serum (FBS), 100 U/mL penicillin, and 100 μg/mL streptomycin. The cell culture related reagents were purchased from Gibco (New York, USA).

2.2. Preparation of co-delivery complexes

2.2.1. Preparation of fluorouracil and PAMAM complexes

PAMAM and fluorouracil were separately dissolved in deionized water. Fluorouracil solution of different concentrations was dropwise added into stirred PG5 solution (concentration of PG5 was 180 μg/mL) and the obtained mixture solution (Fu/PG5) was stirred for a certain duration. Molar ratio of fluorouracil to PG5 (20:1, 100:1 and 200:1), pH value of dissolution medium (pH 5.0, 7.4 and 9.0) and stirring duration (2, 4 and 6 h) were studied to optimize the complexation condition of Fu/PG5, respectively. After stirring, free fluorouracil was removed from the mixture solution by ultrafiltration centrifugation at 3000 rpm (Heraeus Biofuge Stratos, Heraeus Instruments, Osterode, Germany) using a membrane with molecular weight cut-off (MWCO) value of 3000 Da (Millipore, USA). The removed free fluorouracil was quantified using ultraviolet spectrophotometry analysis (UV-2401PC, Shimadzu, Kyoto, Japan). Encapsulation efficiency and drug loading capacity of fluorouracil in Fu/PG5 were calculated based on the determination of free fluorouracil and all experiments were repeated 3 times.

2.2.2. Preparation of co-delivery complexes modified by HA and penetratin

The Dual/PG5 complex was prepared by mixing 100 μL ASO solution (containing 10 μg/mL ASO) with 100 μL Fu/PG5 solution (containing 58.8 μg/mL PG5), leading to a N/P ratio of 8 (PG5/ASO), followed by vigorous vortex (Vortex 3, IKA, Staufen, Germany) for 30 s at room temperature and then standing for 30 min before further use. Then, the Dual/PG5 complex was mixed with 100 μL HA solution (containing HA 20 μg/mL) to obtain Dual/PG5/HA complex, followed by vigorous vortex for 30 s and then standing for 30 min before further use. At final step to form Dual/PG5/HA/Pene complex, 100 μL penetratin solution (containing penetratin 150 μg/mL) was added to Dual/PG5/HA solution following the above-mentioned method.

Fu/PG5/HA/Pene and ASO/PG5/HA/Pene complexes were also prepared according to the same method for scientific assessment (Scheme 1). Fu/PG5/HA/Pene complex was prepared using deionized water instead of ASO solution, and ASO/PG5/HA/Pene complex was prepared using PG5 solution instead of Fu/PG5 solution.

2.3. Characterization of co-delivery complexes

The co-delivery complexes modified with different layers were characterized by dynamic light scattering (DLS) for particle size and zeta-potential using a Zetasizer Nano-ZS (Malvern Instruments, Malvern, UK). Morphology of the complexes was observed under JEM-2100F transmission electron microscope (TEM, JEOL, Tokyo, Japan).

To determine if ASO could be completely condensed into the complexes, these complexes were evaluated by a polyacrylamide gel electrophoresis (PAGE) assay using 12% acrylamide with a voltage of 110 V. The gel was visualized under a chemiluminescent imaging system (FluorChem M, Protein Simple, San Jose, USA) after ASO was stained with GelRed (Biotium, Hayward, USA).

Drug release profiles of the co-delivery complexes were explored *in vitro* using HPLC and fluorescence determination methods. Briefly, fluorouracil and FAM-labeled ASO were used to prepare the complexes, 0.5 mL of which were filled into a dialysis bag (MWCO 20 kD) and immersed in 2.0 mL of 10 mmol/L PBS as release medium at 37 °C. An aliquot of 1 mL release medium was extracted at 10, 30 min, 1, 2, 4, 6, and 8 h, and then equivalent fresh PBS was immediately supplemented. The amount of released fluorouracil was determined by HPLC (Agilent 1100,

Aglient Technologies, Palo Alto, USA) method, with a YMC ODS-A column (4.6 mm × 150 mm, 5 μm) maintained at 20 °C, 2% acetonitrile solution containing 0.1% trifluoroacetic acid as the mobile phase at a flow rate of 0.7 mL/min, and detection wavelength at 214 nm. The amount of released ASO was determined based on the fluorescence intensity of the samples using a Multimode Microplate Reader (Synergy 2, Bio-TEK, Winooski, USA).

2.4. *Cellular uptake of co-delivery complexes*

2.4.1. *Cellular uptake efficiency*

For better evaluation of cellular uptake efficiency, PG5-FITC was used in this experiment instead of PG5 to prepare the complexes, Dual/PG5, Dual/PG5/HA and Dual/PG5/HA/Pene. L929 cells were seeded in a 12-well plate (1×10^5 cells per well) and incubated for 24 h in DMEM medium and 5% CO_2 humidified atmosphere. Cells were then incubated with different complexes containing identical concentration of PG5 (60 μg/mL) for 1 h. FAM solution was used as control. After incubation, the cells were rinsed 3 times with ice-cold PBS (pH 7.4), fixed with 4% paraformaldehyde for 10 min, and imaged by fluorescence microscope (DMI4000 B, Leica, Bensheim, Germany). Besides, quantitative analysis of cellular uptake was determined by a flow cytometer (FACSAria II, BD Bioscience, San Jose, USA) and results were analyzed using Flow Jo software (Treestar Inc., San Carlos, AZ, USA).

2.4.2. *Intracellular distribution*

To observe intracellular distribution of ASO released from the complexes, ASO-FAM was used in this experiment instead of ASO to prepare the three complexes, Dual/PG5, Dual/PG5/HA and Dual/PG5/HA/Pene. L929 cells were seeded in a four-well (6×10^4 cells per well) chambered cover-glass (Lab-Tek) in DMEM and allowed to grow overnight. Cells were then incubated with different complexes containing identical concentrations of PG5 (60 μg/mL) for 4 h. After incubation, cells were rinsed 3 times with ice-cold PBS (pH 7.4), fixed with 4% paraformaldehyde and stained with DAPI before imaging by confocal microscope (LSM710, Carl Zeiss, Jena, Germany).

2.5. *Cytotoxicity evaluation of co-delivery complexes*

Cytotoxicity of the complexes were tested using MTT assay. L929 cells and SDHCEC cells were separately seeded in 96-well plates (3×10^3 cells per well) and incubated for 24 h in DMEM medium and 5% CO_2 humidified atmosphere. Then the medium was refreshed with 200 μL culture medium containing the complexes of different concentrations. SDHCEC cells were treated with Dual/PG5/HA/Pene for cytotoxicity verification. L929 cells were separately treated with free fluorouracil, Fu/PG5, Fu/PG5/HA, Fu/PG5/HA/Pene, ASO/PG5/HA/Pene, Dual/PG5, and Dual/PG5/HA/Pene. For all formulations, drug concentration (ASO and fluorouracil) was normalized according to the concentration of PG5. The highest concentration used in MTT assay containing 180 μg/mL PG5, 20 μg/mL fluorouracil and 30 μg/mL ASO. After 4 h treatment, the cells were cultured with normal medium till 48 h before MTT assay.

2.6. *Anti-fibrosis study of co-delivery complexes on rabbit trabeculectomy model*

2.6.1. *In vivo trabeculectomy model of subconjunctival scarring*

Rabbit model of glaucoma filtration surgery was established as previously described by Gomes Dos Santos et al.[12]. All surgical procedures were performed by an ophthalmologist and all studies were conducted in accordance with guidelines evaluated and approved by the ethics committee of Fudan University (Shanghai, China). New Zealand white rabbits were used to build trabeculectomy models. Rabbits (24 in total) were randomly assigned into 6 groups: normal saline as negative control, intraoperative infiltration with fluorouracil solution (Fu infil.) as positive control, naked ASO, fluorouracil eye drops (Fu dr.), Dual/PG5, Dual/PG5/HA/Pene ($n = 4$). All animals were anesthetized by intramuscular injection of sumianxin II (Shengda Animal Drugs, Dunhua, China) and supplemented with local anesthesia by oxybuprocaine hydrochloride eye drops (Novesine®, Wander Pharma, Nürnberg, Germany) before surgery. Filtration surgery was performed only on the left eye of each experimental rabbit, and was carried out following the standard operation of trabeculectomy. A fornix-based conjunctival flap was created. After mild cauterization of blood vessels, a 3 mm × 3 mm scleral flap of half scleral thickness was dissected. Swabs soaked with either fluorouracil (2.5%, Fu infil. group) or PBS were then applied to the surgical site for 3 min in a masked fashion. Trabeculectomy was performed at the scleral spur, followed by iridectomy. The scleral flap was sutured with 10-0 nylon and Tenon's capsular and conjunctival wound were closed using 8.0 vicryl sutures. Tobramycin and dexamethasone ophthalmic ointment (TobraDex®, Alcon, Fort Worth, TX, USA) was administrated on the left eye after surgery and three times a day during the next 15 days as a prevention of inflammation.

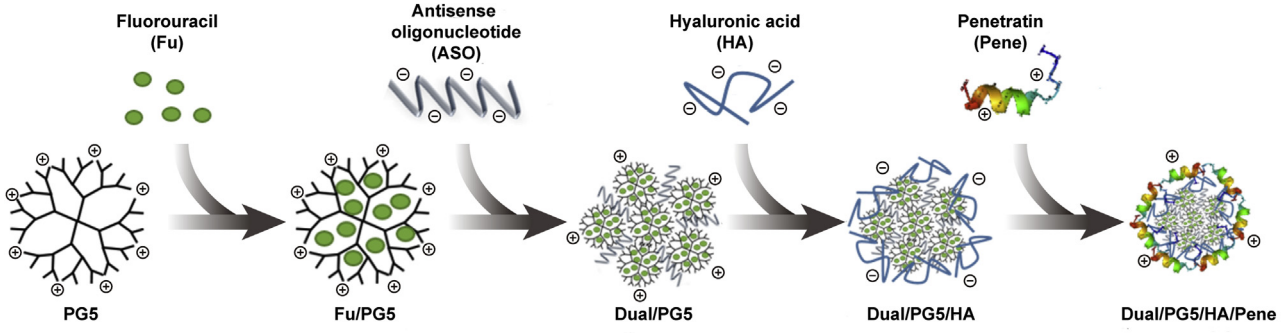

Scheme 1 Schematic diagram showing the preparation process of Dual/PG5/HA/Pene.

2.6.2. Medication and bleb observation

Except the already treated Fu infil. group, the other five groups were separately treated with 50 μL normal saline, fluorouracil solution (containing 20 μg/mL fluorouracil), ASO (containing 30 μg/mL ASO), Dual/PG5 (containing 30 μg/mL ASO and 20 μg/mL fluorouracil), and Dual/PG5/HA/Pene (containing 30 μg/mL ASO and 20 μg/mL fluorouracil) *via* topical instillation three times a day for the following 15 days. Evaluation of filtering blebs was performed by photographic documentation on the 2nd, 4th, 6th, 9th, 12th, and 15th day after surgery. The grading system of filtering bleb was rated according to four indexes: height, vascularity, range, and survival interval. Bleb filtering failure was determined by flat appearance of the bleb and adhesion between the conjunctiva and underlying filtration site.

2.6.3. Histological and immunohistochemistry evaluation

Rabbits were anesthetized and sacrificed with an overdose of pentobarbital sodium after 15 days of treatment. Scleral flap areas of the surgical eye tissues were collected, fixed in 4% paraformaldehyde, dehydrated by graded ethanol and embedded in paraffin, and then 3−4 mm sections were prepared. For histological analysis, the sections were stained with hematoxylin and eosin for general observation of fibrosis tissues and corneal toxicity. The treated slides were observed and imaged under a fluorescence microscope (DMI4000 B, Leica).

For immunohistochemical analysis, tissues were collected and fixed in 10% (*w*/*v*) PBS-buffered formaldehyde and 7 mm sections were prepared with the paraffin embedded tissues. After inactivation of endogenous peroxidase (Beyotime, Shanghai, China), non-specific adsorption was minimized by incubating the sections in normal goat serum (Beyotime). Tissue sections were incubated overnight with primary antibody (rabbit anti-goat, Sangon Biotech, Shanghai, China). Sections were then stained using avidin-biotin methods and the counter stain was developed with diaminobenzidine (Beyotime). Positive staining was marked in brown color, indicating that the immunoreactions were positive[11,18]. The distribution of TGF-β2 was observed using a fluorescence microscope (DMI4000 B, Leica).

2.6.4. Western blotting analysis

Western blotting assay was performed to determine TGF-β2 expression level in fibrosis tissue. To assure accuracy of quantification, each sample contained tissues from all experimental animals in the same group. Surgical sites were excised from eye tissues followed by homogenization and lysis in extraction buffer by sonication on ice. After centrifugation at 4 °C (6000 rpm, Heraeus Biofuge Stratos, Heraeus Instruments), the supernatants were transferred into fresh tubes on ice. Concentrations of isolated proteins were measured using the BCA protein assay kit (Goodbio Technology, Wuhan, China). The protein samples were always kept on ice for subsequent analysis. Equal amounts of total protein were run and separated by 10% SDS-PAGE, and then the proteins were transferred to polyvinylidene difluoride (PVDF) membranes (Millipore, Billerica, MA, USA). The membranes were blocked with 5% non-fat milk in TBST buffer (10 mmol/L Tris-HCl, pH 8.0, 150 mmol/L NaCl, 0.05% Tween-20) and then incubated with primary antibody (1:1000, Sangon Biotech) overnight at 4 °C. Membranes were washed with 1 × TBST buffer (every 5 min, 3 times) and then treated with horseradish peroxidase (HRP) conjugated goat anti-rabbit IgG antibody (Goodbio Technology) at 1:3000 and incubated for 30 min at room temperature, and washed as mentioned above. Blots were visualized and imaged for further analysis (FluorChem M, Protein Simple). The pixel densities in each band were normalized to the amount of glyceraldehyde-3-phosphate dehydrogenase (GAPDH, housekeeping) in that lane.

2.7. Distribution of co-delivery complexes in excised rabbit sclera

Adult New Zealand rabbits were euthanized by an overdose of pentobarbital sodium administered through marginal ear vein. Then the sclera adjacent to corneal limbus were excised and placed vertically between the diffusion cells with epithelium oriented to the donor cell[17]. The mixture of fluorouracil (10 μg/mL) and FAM-labeled ASO (2.5 μg/mL) in 3.5 mL of normal saline or the Dual/PG5/HA/Pene complex containing equivalent fluorouracil and FAM-labeled ASO was added in the donor side, while the acceptor cells contained 3.5 mL normal saline as the diffusion medium, both of which was maintained at 34 ± 0.5 °C by circulating water bath. In order to simulate *in vivo* elimination, an aliquot of 0.5 mL of sample was extracted from the acceptor cell every 0.5 h, following a supplement of 0.5 mL fresh normal saline. After incubation for 2 h, the tissues were fixed in 4% paraformaldehyde and dyed with DAPI for further observation by fluorescent microscope (DMI4000 B, Leica).

3. Results

3.1. Complexation of fluorouracil and PAMAM

In this study, we chose PG5 as the carrier for fluorouracil considering its loading capacity and further application as non-viral gene vector. We investigated the impact of pH value, stirring duration and molar ratio (Fu to PG5) on the encapsulation efficiency (EE) of fluorouracil (Table 1). When complexation was conducted in neutral medium (pH 7.4), the highest EE was achieved. Compared to neutral medium, acidic (pH 5.0) or alkaline (pH 9.0) medium reduced the EE of fluorouracil by 3% and 9%, respectively. The EE of fluorouracil doubled from 12% to 26% when stirring duration extended from 2 to 4 h. Meanwhile, EE only increased 1% when stirring duration extended from 4 to 6 h. The optimization of stirring duration indicated that complexation between fluorouracil and PAMAM approached to equilibrium after stirring for 4 h. Considering both encapsulation rate and dose consumption, molar ratio (Fu to PG5) was set at 100:1.

3.2. Characterization of co-delivery complexes

Morphology observation showed that all the complexes were in spherical shape and at nanoscale sizes (Fig. 1). Compared to the Dual/PG5 complex, TEM image of the Dual/PG5/HA complex showed a clearly semitransparent polysaccharide layer surrounding the particle, which indicated HA has been successfully coated on the outer surface of the complex (Fig. 1A). The HA coating has also been verified by zeta potential analysis. Zeta potential of Dual/PG5/HA reversed to −8.7 mV in contrast with +21.9 mV of Dual/PG5, which indicated that HA had shielded the excessive amino groups of PG5 (Fig. 1B). After addition of penetratin layer, zeta potential value of Dual/PG5/HA/Pene increased to +4 mV and the complex exhibited uniform texture under TEM. The particle size of Dual/PG5 complex was around 125 nm. Coating with HA layer led to a significant increase in the particle size of Dual/PG5/HA to approximately 200 nm. When penetratin was further

absorbed on the surface, the particle size of formed Dual/PG5/HA/Pene complex decreased to about 100 nm. These results implied that not only the HA layer was highly compressed by positively charged penetratin, but also the complexes might be reassembled during penetratin insertion.

In vitro release profiles of fluorouracil and ASO were illustrated in Fig. 1C and D, respectively. Fluorouracil was released significantly slower from the Dual/PG5/HA/Pene complex, compared with the solution, primary complex Dual/PG5, and even intermediate complex Dual/PG5/HA. The accumulative amounts of released fluorouracil ranged from 30.65% to 72.19% during initial 10 min and 2 h, which was about 20% less ($P < 0.01$) than those from fluorouracil solution. Considering after administration the retention time of conventional eye drop is only several minutes in the conjunctival sac, the sustained-release characteristics of Dual/PG5/HA/Pene complex would be sufficient for topical absorption of fluorouracil. In contrast, only naked ASO could be released into the medium within 8 h *in vitro*, revealing that all the complexes could provide complete protection for ASO.

3.3. Cellular uptake of co-delivery complexes

FITC was conjugated to PG5 as a tracer of the complexes, and then cellular uptake of the complexes was evaluated qualitatively and quantitatively. From the fluorescent images (Fig. 2A), it could be clearly seen that the cells showed the strongest green fluorescence when treated with Dual/PG5/HA/Pene complex. Quantitative results from flow cytometer analysis further confirmed this observation. Even though the uptake percentage by L929 cells had almost no statistically significant difference among these experimental groups (Fig. 2B), the mean fluorescence intensity significantly increased with each additional layer of the complexes (Fig. 2C). Compared with Dual/PG5 and Dual/PG5/HA, the mean fluorescence intensity of Dual/PG5/HA/Pene treated cells increased about 3-fold and 2-fold, respectively.

3.4. Intracellular distribution

Antisense oligonucleotide specific for TGF-β2 was covalently labeled by FAM (green color) to trace the distribution of co-delivery complexes in L929 cells (Fig. 3). Lysosomes were stained by LysoTracker® (red color) for better presentation of the intracellular localization of ASO.

As hydrophilic macromolecule, naked ASO was inefficient to pass through cell membranes, and therefore few naked ASO (green) could be found in the L929 cells. When condensed by PG5, Dual/PG5 was internalized into the cells and trapped in red endosomes, leading to merged yellow color in cytoplasm. Similar to Dual/PG5, Dual/PG5/HA was also trapped in lysosomes in the cells at a slightly higher concentration. Obviously different with the above two complexes, only few Dual/PG5/HA/Pene co-localized with lysosomes. Most of Dual/PG5/HA/Pene was found in the cytoplasm, as presented by the green color in the fluorescence-merged image.

3.5. Inhibition on cellular proliferation

To verify that the modification layers improved delivery efficacy of the complexes, fluorouracil was loaded in different complexes for comparison of their cytotoxicity (Fig. 4A). L929 cells were treated with free fluorouracil solution, Fu/PG5, Fu/PG5/HA, and Fu/PG5/HA/Pene complexes, respectively. Each formulation contained same amount of fluorouracil for parallel comparison. Under high concentration of 90 μg/mL PG5 [Lg(PG5) = 1.95], inhibition rate of cell viability was about 40% in free fluorouracil and Fu/PG5/HA treated groups, and about 90% in Fu/PG5 and Fu/PG5/HA/Pene treated groups. Under low concentration of 11.2 μg/mL PG5 [Lg(PG5) = 1.05], inhibition rate of cell viability was about 10% in free fluorouracil, Fu/PG5, and Fu/PG5/HA treated groups, and about 40% in Fu/PG5/HA/Pene treated groups. To further confirm the enhanced cytotoxicity of double-layer modified complexes, L929 cells were treated with Dual/PG5 and Dual/PG5/HA/Pene complexes, respectively. The results in Fig. 4B revealed a significantly increased cytotoxicity in Dual/PG5/HA/Pene treated group under lower concentration. The calculated IC_{50} of Dual/PG5 and Dual/PG5/HA/Pene complexes were 28.3 μg/mL PG5 and 14.5 μg/mL PG5, respectively.

To explore whether the inhibition efficacy could be improved by the synergistic effect of ASO and fluorouracil, L929 cells were treated with ASO/PG5/HA/Pene, Fu/PG5/HA/Pene, and Dual/PG5/HA/Pene, respectively (Fig. 4C). The complexes only loaded with nucleic acid (ASO/PG5/HA/Pene) exhibited almost no cytotoxicity on L929 cells. The complexes only loaded with chemical drug (Fu/PG5/HA/Pene) inhibited about 50% cells under concentration of 90 μg/mL PG5 [Lg (PG5) = 1.95]. The co-delivery complexes (Dual/PG5/HA/Pene) showed the highest inhibition rate of cell proliferation and inhibited about 75% fibroblast cells under the same concentration. The calculated IC_{50} of Fu/PG5/HA/Pene and Dual/PG5/HA/Pene complexes were 36.4 μg/mL PG5 and 14.5 μg/mL PG5, respectively. SDHCEC cells and L929 cells were both treated with Dual/PG5/HA/Pene to assess the cytotoxicity on target cells and normal ocular cells (Fig. 4D). MTT assay showed that the cytotoxicity of Dual/PG5/HA/Pene complex on corneal cells was reduced by 50% compared with that on fibroblast cells. More importantly, under concentration of 11.2 μg/mL PG5 [Lg(PG5) = 1.05], Dual/PG5/HA/Pene complex inhibited about 50% L929 cells while showed no cytotoxicity on SDHCEC cells.

3.6. Anti-fibrosis on rabbit trabeculectomy models

3.6.1. Morphology observation of filtering blebs

The trabeculectomy models were established according to the standard surgical protocol using New Zealand white rabbits to evaluate the fibroblast inhibition effect of the co-delivery

Table 1 Optimization of complexation factors in preparation of Fu/PG5.

Complexation	pH			Time (h)			Molar ratio (Fu to PG5)		
Factors	5.0	7.4	9.0	2	4	6	20	100	200
EE (%)	14.8 ± 1.2	17.8 ± 0.8	8.8 ± 1.2	12.3 ± 0.4	26.4 ± 0.3	27.8 ± 0.2	46.8 ± 0.2	25.8 ± 0.3	17.6 ± 0.4
DLC (%)	7.2 ± 0.4	9.1 ± 0.2	4.5 ± 0.1	4.9 ± 0.1	10.1 ± 0.5	11.6 ± 0.4	3.7 ± 0.1	9.8 ± 0.3	10.2 ± 0.3

Data are mean ± SD, $n = 3$. EE, encapsulation efficiency; DLC, drug loading capacity.

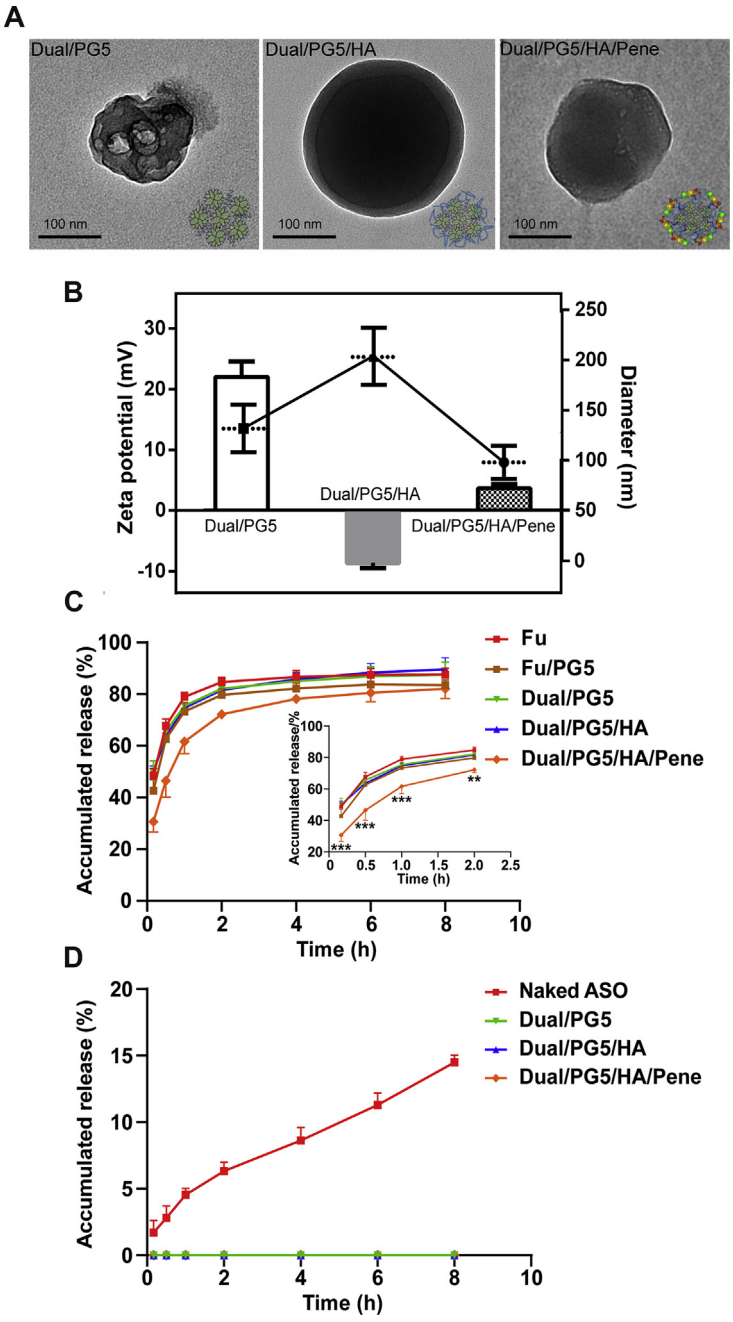

Figure 1 (A) TEM photographs of Dual/PG5, Dual/PG5/HA and Dual/PG5/HA/Pene complexes. Corresponding schematics were displayed in the corner of each image. (B) Zeta potentials and particle sizes of the complexes. Release profiles of fluorouracil (C) and FAM-labeled ASO (D) from various complexes into 10 mmol/L PBS (pH7.4) at 37 °C. Data are represented as mean ± SD, $n = 3$. Statistical significance was determined by analysis of variance using the Tukey method, $^{**}P < 0.01$, $^{***}P < 0.001$ compared with fluorouracil solution (Fu).

complexes (Supporting Information Fig. S1). Because of surgical trauma, there was a high propensity of subconjunctival fibrous tissue formation during postsurgical healing, which could be identified by morphology observation of the filtering blebs. The proliferative phase of wound healing begins at 1−3 days following surgery, and it usually takes 8−12 days before successful wound healing with functional filtering blebs[19]. Therefore, observations were performed in the following 15 days after surgery. The Indiana Bleb Appearance Grading Scale (IBAGS) was adopted to classify the filtering blebs after trabeculectomy[20]. According to the criteria stipulated in IBAGS (Supporting Information Table S1), morphologic parameters of the filtering blebs such as bleb height, bleb extent, and vascularity were evaluated, and survival intervals of the blebs were also recorded.

Filtering bleb is referring to the elevated subconjunctival space in the eye and its height is determined by aqueous humor draining from the anterior chamber *via* previously created surgical passage. The formation and developing progress of filtering blebs could be observed in photograph records. As exhibited in Fig. 5A, the filtering blebs first emerged as small cystic forms and gradually flattened into applanate forms while preserving their filtering function. Therefore, the height and extent of the blebs represented

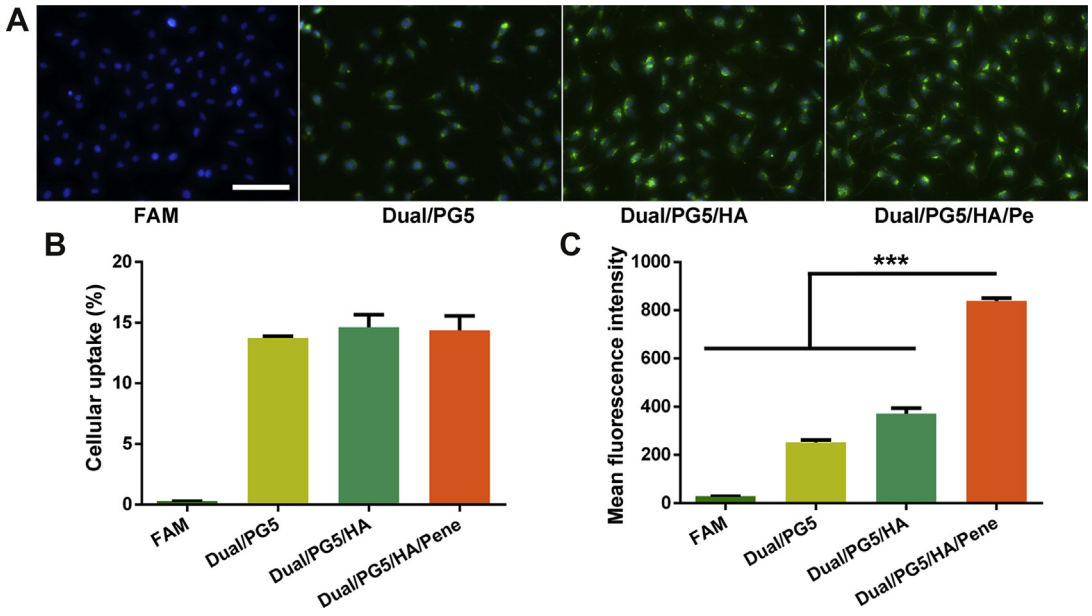

Figure 2 Cellular uptake of co-delivery complexes by L929 cells. Fluorescence-labeled PG5 was used to prepare the complexes. Cells were incubated with each complex for 1 h before analysis. Free fluorescence probe was used as control. (A) Representative fluorescence images of the complexes. Green and blue signals are from the complex core (PG5-FITC) and cell nucleus (DAPI), respectively. Quantitative results were analyzed by flow cytometer (B) cellular uptake percentage and (C) mean fluorescence intensity were displayed (mean ± SD, $n = 3$). Statistical significance was determined by analysis of variance using the Holm-Sidak method, $^{***}P < 0.001$. Scale bar, 100 μm.

their filtering efficiency and the blebs would be defined as dysfunction when adhesion occurred between the conjunctiva and underlying filtration site. Results revealed that the group treated with Dual/PG5/HA/Pene was able to maintain bleb height and extent without significant difference from positive control group (Fig. 5B and C). Meanwhile, the groups treated with normal saline, naked ASO, free fluorouracil, and Dual/PG5 were successively determined as failure blebs from day 9 to day 15, although Dual/PG5 complex exhibited a slight advantage among them.

After tissue trauma induced by surgery procedures, activated platelets along with fibrinogen and fibronectin began to accelerate coagulation, at the same time, they provided a short-term structural support for proliferation of inflammatory cells, vascular endothelial cells and fibroblast cells[21,22]. Therefore, degree of congestion indicated the propensity of fibroblast scars, and vascularity foreshadowed potential failure of blebs. We found that there was no significant difference in vascularity between all the groups, and all the filtering blebs presented avascular status at the endpoint of observation (Fig. 5D). This result revealed that the formulations induced almost no inflammation response and all the treated eyes were in normal healing condition.

In consistence with the morphologic observation of the blebs, survival interval analysis showed that the groups treated with Dual/PG5/HA/Pene and positive control were able to prolong bleb survival following trabeculectomy compared to the other groups, preserving 75% functional filtering blebs after 15 days of observation (Fig. 5E). Since wound healing is generally considered completed after 12 days following trabeculectomy, the preserved blebs were expected with long-term function.

3.6.2. *Histological observation*

Ocular tissues, including surgical site and corneal area, were processed using hematoxylin and eosin staining method to observe inflammatory response and scar formation. Scar tissues were stained in violet and circled by dash line to show the area of surgical incision (Fig. 6A). This visualized result provided an intuitive criterion to determine the outcome of trabeculectomy. Distinctive difference could be seen from Fig. 6A that Dual/PG5/HA/Pene complex showed an obvious inhibitory effect on scar formation. Fibroblasts were scarce and formed monolayer surrounding the surgical site of Dual/PG5/HA/Pene treated group as well as of the positive control group. While in the other experimental groups, fibroblasts spread in an extensive area around surgical site. There were also few collagen fibers (shown in the circled area) around scar tissues in the Dual/PG5/HA/Pene and Fu (infil.) treated groups, suggesting slighter collagen deposition and better filtering function. In the other experimental groups, there was densely packed mature collagen deposition, indicating formation of pathological cicatrization and dysfunctional filtering blebs[23,24].

In all the histological observations on the surgical sites and corneas, no sign of inflammation was found, and neighboring eye tissues such as sclera and limbus were neither involved in the inflammatory processes, suggesting that the complexes were of good biocompatibility. Especially, no corneal injury was observed as shown in Fig. 6B, which was consistent with the result of our previous MTT assay that Dual/PG5/HA/Pene complex was safe to corneal cells and it could be administrated *via* instillation without harming corneal tissue.

3.6.3. *TGF-β2 expression in filtering regions*

Surgical sites were subsequently examined for their TGF-β2 expression using immunohistochemical staining for qualitative observation and using western blotting for quantitative analysis. As shown in Fig. 7A, since surgical wounds were induced by operation, TGF-β2 was activated and stained in brown dots within microscopic field. Comparing TGF-β2 expression in filtering sites of the other groups, the groups treated with Dual/PG5/HA/Pene

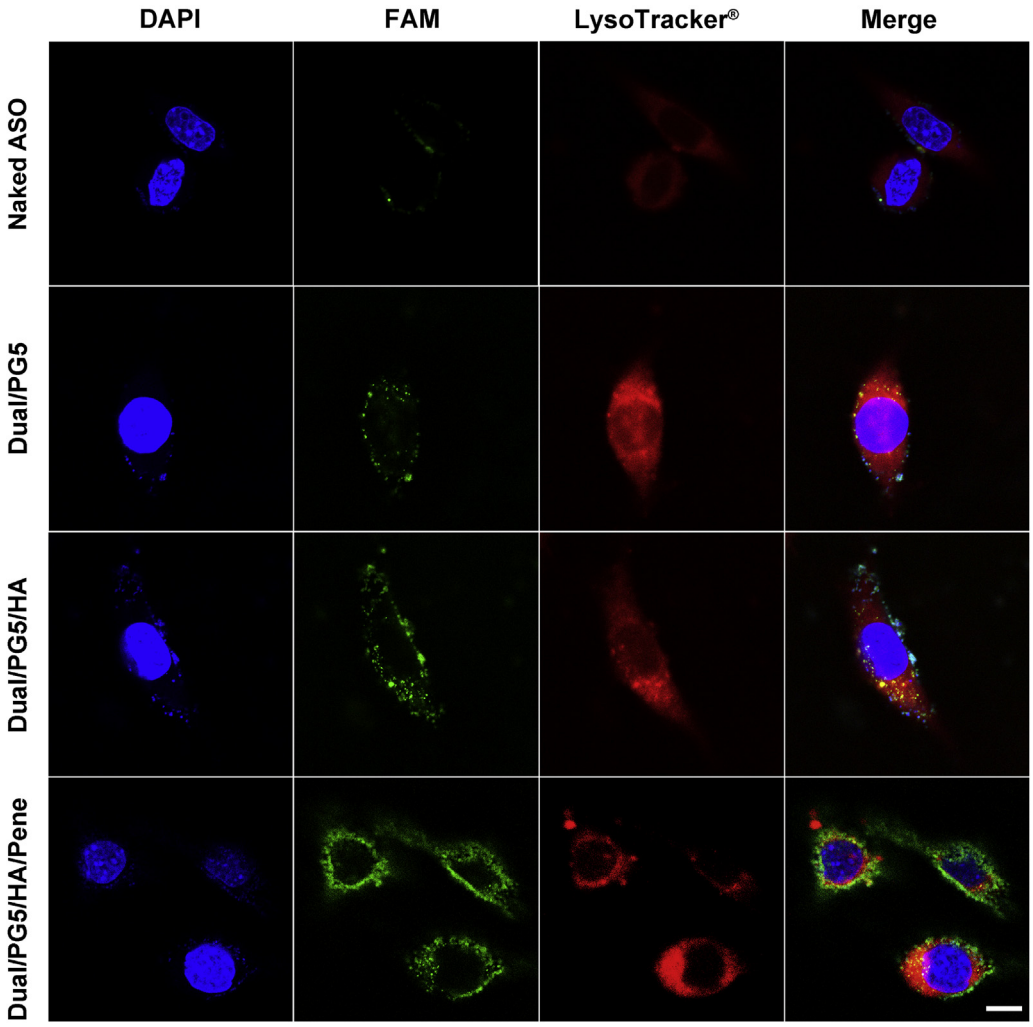

Figure 3 Confocal microscope images exhibit intracellular distribution of ASO. Fluorescence-labeled ASO was used to prepare the complexes. L929 cells were incubated with naked ASO and the complexes for 4 h before analysis. Green represents ASO (ASO-FAM), blue represents cell nuclear (DAPI), red represents lysosomes (lysotracker), and yellow represents a merged area of green and red. Scale bar, 20 μm.

and Fu (infil.) exhibited lighter and sparser stains, as circled by dash line.

For accurate quantification, each sample analyzed in western blotting assay contained tissues from the same group (Fig. 7). Since TGF-β2 exists in cells as a non-activated isoform and would be activated by tissue trauma or stress response[25], we added an untreated group without surgical procedure to define the baseline of normal expression level of TGF-β2. Electrophoretic bands were shown in Fig. 7B, which presented that normal cells without tissue trauma expressed little TGF-β2. However, the expression level of TGF-β2 dramatically increased over 20-fold after trabeculectomy (Fig. 7C). In all the testing groups, TGF-β2 expressions were inhibited compared to that in normal saline treated group. It was worth noting in Fig. 7D that compared to saline treated group, the relative expression amount of TGF-β2 in Dual/PG5/HA/Pene treated group was only around 45%, especially considering the same index was about 50% in Fu (infil.) treated group (positive control). Meanwhile, the relative expression amount of TGF-β2 in the other experimental groups ranged from 55% to 70% within obvious scar areas. Taken together, from the results of immunohistochemical staining and western blotting, Dual/PG5/HA/Pene complex was the most efficient in inhibiting TGF-β2 expression.

4. Discussion

Trabeculectomy is a common surgical treatment of glaucoma, which can help to decrease intraocular pressure *via* aqueous humor drainage. A functional filtering passage can be built after trabeculectomy by removing part of the trabecular meshwork and iris. The success rate of trabeculectomy depends on the survival of functional filtering blebs. There is a probability of filtering bleb failure when scarring occurs due to fibroblast over proliferation. In this study, we combined gene therapy (ASO specific for TGF-β2) with chemical drug (fluorouracil) in a co-delivery system, aiming to inhibit fibroblast proliferation *in vivo via* a noninvasive method. In order to achieve this objective, an efficient delivery system with enhanced drug-loading capacity and ocular tissue-penetrating ability was indispensable.

It has been reported that fluorouracil could spontaneously bind with the protonated superficial amine groups of PAMAM−NH_2, and could also interact with the non-protonated superficial or internal amine groups of PAMAM−NH_2[9]. The combination ability of PAMAM with fluorouracil depends on the surface groups and generation of PAMAM. Experiments showed that fluorouracil-loading capacity was higher with cationic PAMAM−NH_2

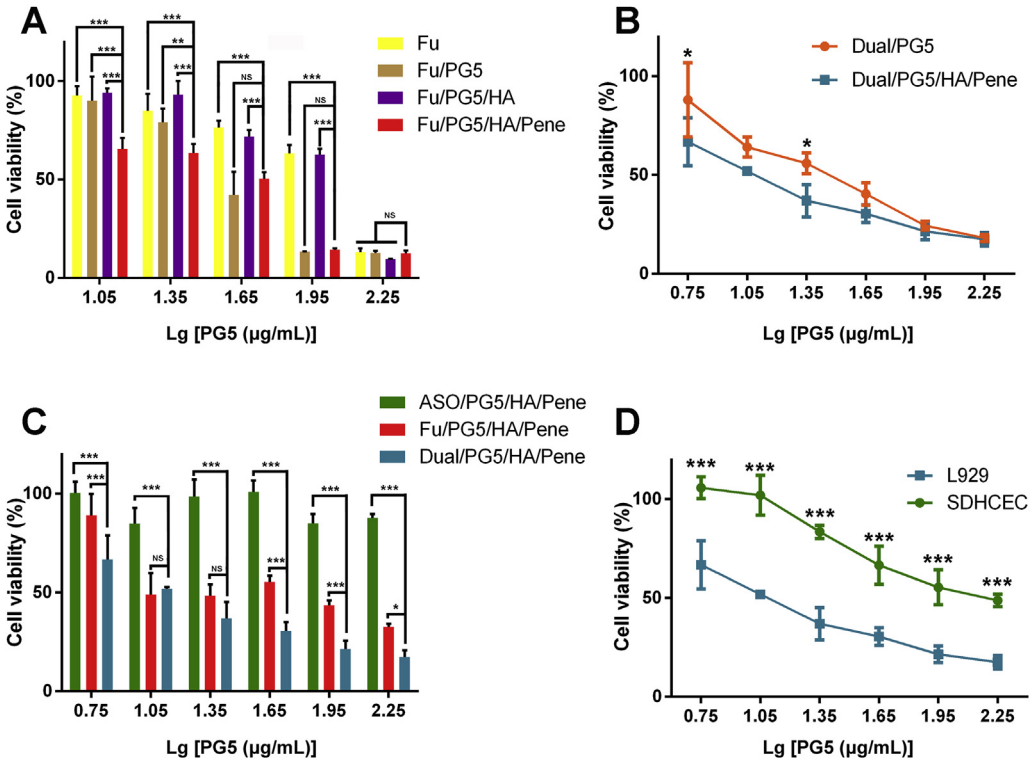

Figure 4 *In vitro* cytotoxicity evaluation of the complexes. (A)−(C) Viability of L929 cells after 4 h incubation with different formulations determined by MTT assay. (D) Viability comparison between L929 cells and SDHCEC cells after 4 h incubation with the co-delivery complex determined by MTT assay (mean ± SD, $n = 3$). Statistical significance was determined by analysis of variance using the Holm-Sidak method, NS, $P > 0.05$, $^{*}P < 0.05$, $^{**}P < 0.01$, $^{***}P < 0.001$.

dendrimer than with the hydroxyl analog PAMAM−OH[26]. There is also a positive correlation between fluorouracil-loading capacity and the generation of PAMAM, which is reasonable because higher generation contains more binding sites[27]. Therefore, we chose the fifth generation of PAMAM−NH_2 dendrimer as carrier core for the co-delivery system.

In order to build a co-delivery system with enhanced penetrating ability, we further modified the Dual/PG5 complex with HA and penetratin. From morphology observation, it could be seen that HA coating increased the particle size of Dual/PG5/HA complex, whereas addition of penetratin decreased particle size by almost half. This could be attributed to the abundant positive charges of penetratin, which neutralized the negative charges of HA and consequently compressed the HA layer. As a result, the uniform texture of Dual/PG5/HA/Pene could be seen in the TEM image compared to the obvious HA layer of Dual/PG5/HA. Meanwhile, fluorouracil loaded in the Dual/PG5/HA/Pene complex displayed a sustained-release characteristic, mainly due to the compact coating layer composed of both HA and penetratin. The electrostatic interaction between negatively charged ASO and positively charged PAMAM was competent to prevent pre-release of ASO *in vitro*, which was also proved by the PAGE results (Supporting Information Fig. S2).

The enhanced penetrating ability of modified complexes was verified in cellular uptake experiments. The uptake percentage of Dual/PG5, Dual/PG5/HA and Dual/PG5/HA/Pene were nearly the same and would increase with incubation time in theory. While in this study, the cells were incubated with the complexes for only 1 h in consideration of its application *via* topical instillation. It is worth noting that mean fluorescence intensity significantly increased when the complex was modified with both HA and penetratin. This result revealed that the penetrating ability of the complexes was endowed by the additional layers.

Firstly, we modified the Dual/PG5 complex with HA layer and the resulting Dual/PG5/HA complex accumulated more in the cells. Since hyaluronic acid is an endogenous component with great biocompatibility and bioadhesive property, it may provide a prolonged contacting time between the complex and cytomembrane[28]. This facilitated internalization of the complex because hyaluronic acid receptor was highly expressed on the surface of fibroblast cells[29,30], although addition of HA had reversed the electrical potential of the complex.

When the complex was further modified with penetratin, mean fluorescence intensity in L929 cells significantly increased twice than the Dual/PG5/HA complex after co-incubation. Penetratin is a cell-penetrating peptide with good ocular permeability, which has been validated in our previous work[17]. In the Dual/PG5/HA/Pene complex, penetratin bound to the HA layer on the outer surface of Dual/PG5/HA complex through electrostatic interaction. More specifically, the positively charged residues of penetratin were electrostatically attracted to the negatively charged carboxyl of HA. However, penetratin still enhanced the uptake efficiency of Dual/PG5/HA/Pene complex, indicating that electrostatic interaction did not impair the membrane permeability of penetratin. This was consistent with our previous speculation that the penetrating ability of penetratin was partially due to its hydrophobicity[31].

The increased uptake efficiency of Dual/PG5/HA/Pene was also observed in confocal microscopy images. These images squared with what we already knew about the uptake pathway of

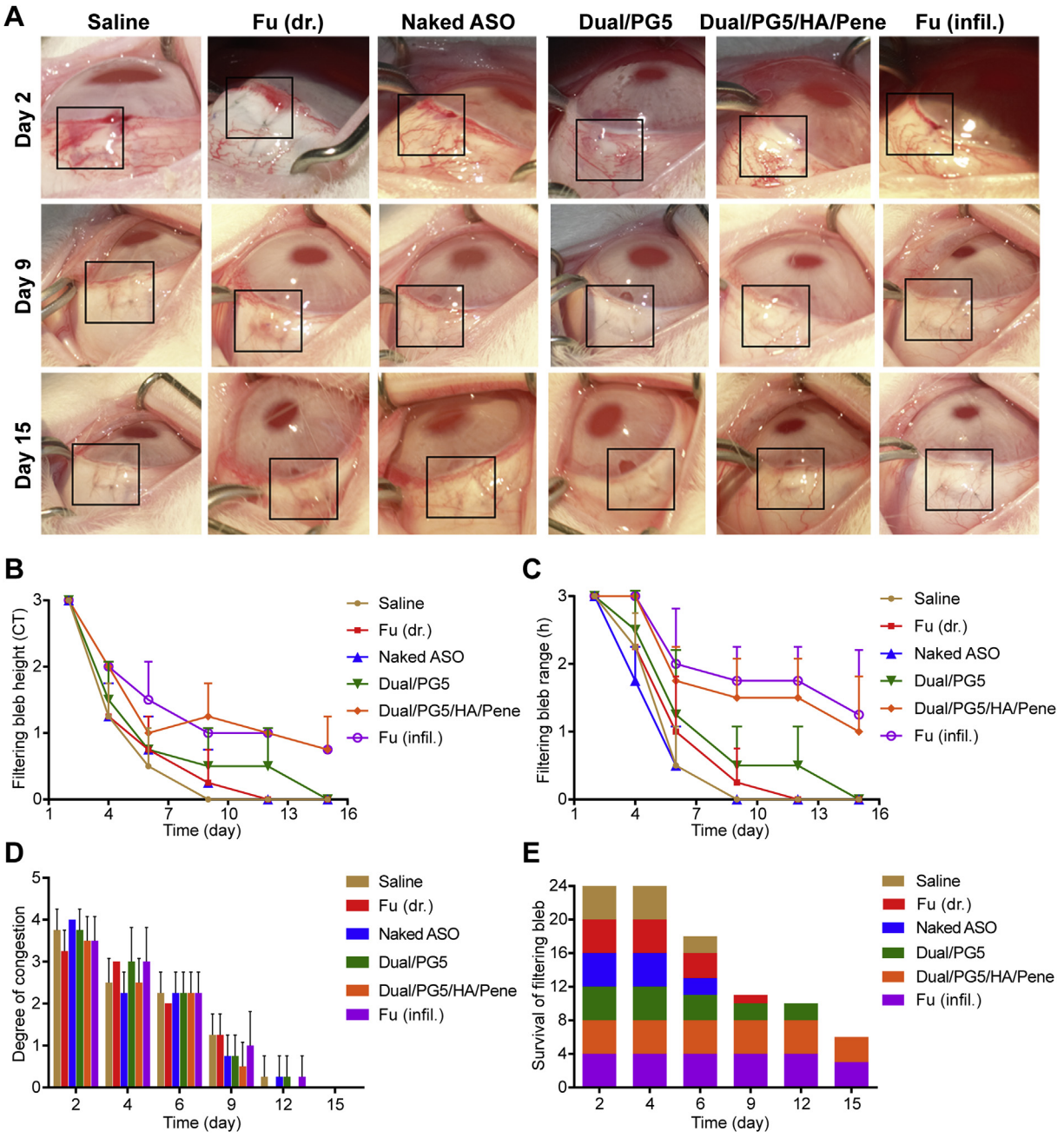

Figure 5 Morphological evaluation on filtering blebs from day 2 to day 15 after trabeculectomy. (A) Morphology observation. Filtering bleb areas are marked with black lines. Rabbits were operated on one-side eye and treated 3 times a day with saline, fluorouracil [Fu (dr.)], naked ASO, Dual/PG5, and Dual/PG5/HA/Pene complexes. The positive control group [Fu (infil.)] was only treated with fluorouracil infiltration for 3 min during surgery and no more additional treatment was implemented during following observation. Filtering blebs were evaluated for (B) filtering bleb height (C) filtering bleb range, and (D) degree of congestion according to the grading system ($n = 4$), paralleled to height, extent and vascularity parameters in the IBAGS, respectively. (E) Survival analysis is displayed and the height of each square represents the number of remaining functional filtering blebs ($n = 4$).

PAMAM, which was generally internalized by endocytosis and escaped from lysosomes through proton sponge mechanism[32]. When coated with HA layer, intracellular distribution of Dual/PG5/HA complex increased than that of Dual/PG5, which may be due to the hyaluronic acid receptor on the surface of L929 cells and the enhanced cell adhesion mediated by HA. After adding the penetratin layer, the complexes could be seen diffused in cytoplasm as well as in lysosomes. It has been found that except for improving internalization, cell-penetrating peptide could also play an important role in releasing nucleic acids by disrupting endolysosomes[33,34]. There were also studies showing that a direct translocation through the cell membrane was more likely to occur when the cell-penetrating peptide was complexed with cargoes[35,36]. Based on these theories, it was reasonable to deduce that the improvement of endocytosis and release of both drugs (fluorouracil and ASO) was owing to the addition of penetratin.

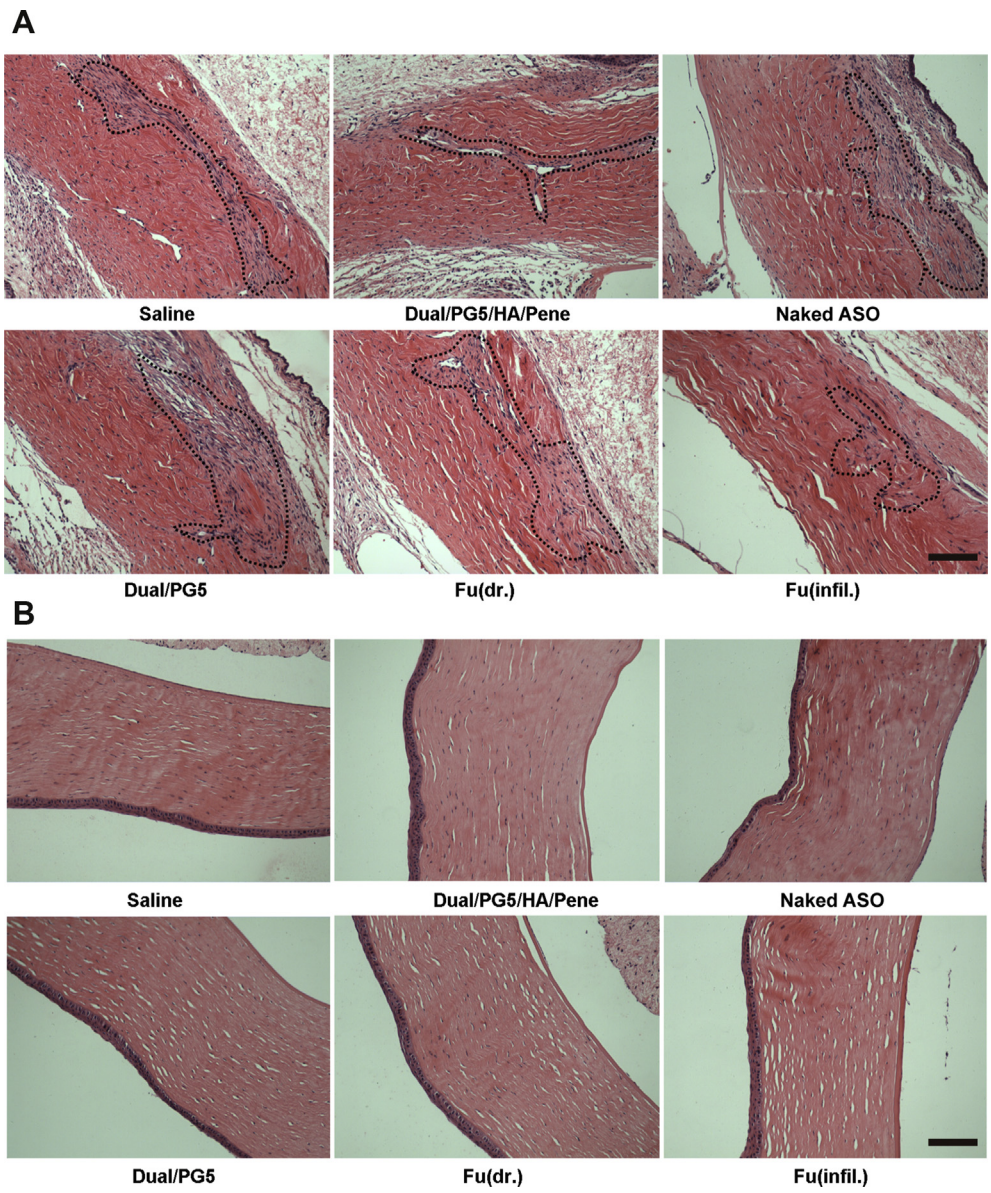

Figure 6 Anti-fibrosis efficiency of the co-delivery complexes. Rabbits were sacrificed 15 days after filtering surgery, eye tissues were collected, fixed, dehydrated, and embedded in paraffin. Tissues were cut into 3−4 μm sections for hematoxylin−eosine staining. (A) Fibrosis tissues (circled with black dot lines) in filtering areas and (B) tissue toxicity in corneas was observed under microscope. Scale bar, 200 μm.

The following cytotoxicity tests showed that the modified complexes behaved better at inhibiting proliferation of fibroblast cells. When treated with the complex only coated with HA, inhibition efficiency was negligible, although the previous cellular uptake study showed an improved internalization of the HA modified complex. When the functional proton-sensitive surface of PAMAM was coated with HA, the complex was hard to benefit from proton sponge effect and the encapsulated drugs were unlikely to be released into cytoplasm. When modified with both HA and penetratin, the complex would not only exhibit an improved cell-penetrating efficiency but also increase the inhibition efficiency on L929 cells. The same tendency could be found in Fu/PG5/HA/Pene treated group as well as in Dual/PG5/HA/Pene treated group. This finding was consistent with the result that intracellular distribution of Dual/PG5/HA/Pene in cytoplasm was more than that of Dual/PG5 and Dual/PG5/HA.

Compared to the complexes carrying only ASO or fluorouracil, the co-delivery complex showed the highest inhibition efficiency on proliferation of L929 cells. This revealed the possibility that ASO and fluorouracil worked synergistically and addition of ASO could reduce the fluorouracil dose and consequently the potential toxicity and side effects. TGF-β2 exists in cells in a non-activated isoform under normal circumstances, and can be activated when the microenvironment is acidized or in the presence of protein cleavage[37]. So it was reasonable to deduce that when fluorouracil and ASO were delivered into cells simultaneously, DNA synthesis was blocked by weakly acidic drug fluorouracil, and further a weak acidic intracellular microenvironment was created to activate TGF-β2. ASO would further consolidate the inhibition effect of fluorouracil with antisense effect on TGF-β2. The inhibition ability of Dual/PG5/HA/Pene was confirmed in the following observation on the animal models of trabeculectomy. After treated

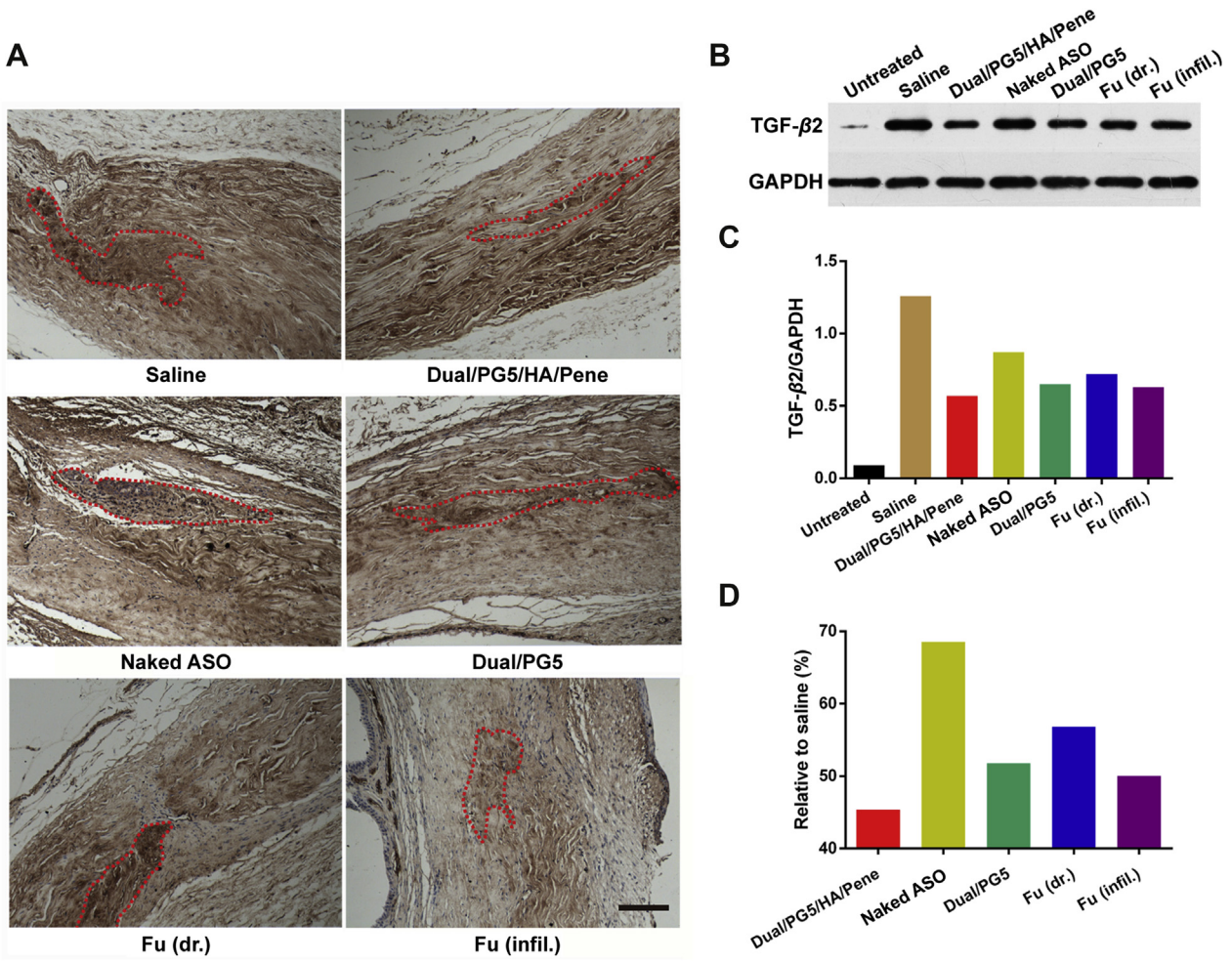

Figure 7 Inhibition effect of TGF-β2 expression by co-delivery complexes. Rabbits were sacrificed 15 days after filtering surgery. (A) Eye tissues were collected, fixed, dehydrated, and embedded in paraffin. Tissues were cut into 3−4 μm sections for immunohistochemical staining. TGF-β2 was stained as dark brown (circled with red dot lines) for microscopic observation. Quantitative analysis of surgical areas, where the same size tissues were collected and processed with standard Western blot procedures. (B) Western blot bands of TGF-β2 expression (C) quantitative absorbance values of each band and (D) inhibition efficiency of all the testing groups analyzed relative to the normal saline treated group. Scale bar, 200 μm.

by the co-delivery complex, both proliferation of fibroblasts and expression of TGF-β2 were inhibited.

Based on the results of *in vitro* experiments, we tested the inhibition efficiency of the co-deliver system we developed on *in vivo* scar formation. The comprehensive evaluation of anti-fibrosis on rabbit trabeculectomy models indicated that Dual/PG5/HA/Pene succeeded in inhibiting postoperative fibrosis proliferation, probably due to improved permeability of the complex in sclera (Supporting Information Fig. S3). This inhibition efficiency was not only consistent with the positive control [Fu (infil.) treated group], but also non-toxic to normal eye tissues. Considering the rate of scar formation in rabbits was faster than in humans, the application of Dual/PG5/HA/Pene complex in postoperative scarring was quite optimistic.

5. Conclusions

In summary, a novel and efficient approach employing co-delivery strategy had been proposed to prevent post-trabeculectomy scar formation. Complexes against fibroblast proliferation was designed based on dendrimer core to carry fluorouracil as well as to condense anti-TGF-β2 ASO. With the aid of further modification by HA and penetratin, the co-delivery complex showed efficient cellular uptake and consequently improved intracellular distribution and enhanced cytotoxicity on fibroblast cells. By taking advantage of the ocular permeability of penetratin, Dual/PG5/HA/Pene complex exhibited equivalent fibrosis inhibition efficiency with fluorouracil infiltration, the positive control applied in clinic, in the trabeculectomy animal model. *In vitro* and *in vivo* studies demonstrated that fluorouracil and anti-TGF-β2 ASO exerted a strengthened synergistic effect on inhibition of scar formation, which provided useful clinic-relevant information for combination medication. In addition, Dual/PG5/HA/Pene complex was administered through noninvasive method to minimize the injury to normal ocular tissues, which may greatly improve patient convenience and compliance compared with currently intraoperative treatment and postoperative injection. This work had demonstrated a promising noninvasive treatment for postoperative fibroblast proliferation and showed potential to increase the success rate of trabeculectomy.

Acknowldgments

This study was supported by funding from the National Natural Science Fund of China (Grant Nos. 81573358, 81172994, 81690263 and 81773670), and the Development Project of Shanghai Peak Disciplines-Integrative Medicine (20180101, China).

Author contributions

Kuan Jiang, *in vitro* release and *ex vivo* permeability of the complexes, data presentation and manuscript preparation; Junyi Chen, establishment of the trabeculectomy animal model; Lingyu Tai, construction and *in vitro* evaluation of the complexes, data summary; Chang Liu, *in vitro* characterization of the complexes; Xishan Chen, *in vivo* pharmacodynamic evaluation; Gang Wei, experiment design, data interpretation, drafting the work; Weiyue Lu, participation in experiment design; Weisan Pan, participation in data interpretation.

Conflicts of interest

There is no conflict of interest among all authors contributed to this research.

Appendix A. Supporting information

Supporting data to this article can be found online at https://doi.org/10.1016/j.apsb.2020.03.002.

References

1. Davis BM, Crawley L, Pahlitzsch M, Javaid F, Cordeiro MF. Glaucoma: the retina and beyond. *Acta Neuropathol* 2016;**132**:807–26.
2. Quigley HA, Broman AT. The number of people with glaucoma worldwide in 2010 and 2020. *Br J Ophthalmol* 2006;**90**:262–7.
3. Klink T, Rauch N, Klink J, Grehn F. Influence of conjunctival suture removal on the outcome of trabeculectomy. *Ophthalmologica* 2009;**223**:116–23.
4. Landers J, Martin K, Sarkies N, Bourne R, Watson P. A twenty-year follow-up study of trabeculectomy: risk factors and outcomes. *Ophthalmol Times* 2012;**119**:694–702.
5. Schlunck G, Meyer-ter-Vehn T, Klink T, Grehn F. Conjunctival fibrosis following filtering glaucoma surgery. *Exp Eye Res* 2016;**142**:76–82.
6. Mochizuki K, Jikihara S, Ando Y, Hori N, Yamamoto T, Kitazawa Y. Incidence of delayed onset infection after trabeculectomy with adjunctive mitomycin C or 5-fluorouracil treatment. *Br J Ophthalmol* 1997;**81**:877–83.
7. Yavuz B, Pehlivan SB, Vural I, Unlu N. *In vitro/in vivo* evaluation of dexamethasone-PAMAM dendrimer complexes for retinal drug delivery. *J Pharm Sci* 2015;**104**:3814–23.
8. Wang WY, Yao C, Shao YF, Mu HJ, Sun KX. Determination of puerarin in rabbit aqueous humor by liquid chromatography tandem mass spectrometry using microdialysis sampling after topical administration of puerarin PAMAM dendrimer complex. *J Pharmaceut Biomed Anal* 2011;**56**:825–9.
9. Buczkowski A, Waliszewski D, Urbaniak P, Palecz B. Study of the interactions of PAMAM G3–NH_2 and G3–OH dendrimers with 5-fluorouracil in aqueous solutions. *Int J Pharm* 2016;**505**:1–13.
10. Delplace V, Payne S, Shoichet M. Delivery strategies for treatment of age-related ocular diseases: from a biological understanding to biomaterial solutions. *J Contr Release* 2015;**219**:652–68.
11. Cordeiro MF, Gay JA, Khaw PT. Human anti-transforming growth factor-beta2 antibody: a new glaucoma anti-scarring agent. *Invest Ophthalmol Vis Sci* 1999;**40**:2225–34.
12. Gomes Dos Santos AL, Bochot A, Doyle A, Tsapis N, Siepmann J, Siepmann F, et al. Sustained release of nanosized complexes of polyethylenimine and anti-TGF-β2 oligonucleotide improves the outcome of glaucoma surgery. *J Contr Release* 2006;**112**:369–81.
13. Chen H. Recent developments in ocular drug delivery. *J Drug Target* 2015;**23**:597–604.
14. Barar J, Aghanejad A, Fathi M, Omidi Y. Advanced drug delivery and targeting technologies for the ocular diseases. *Bioimpacts* 2016;**6**:49–67.
15. Group Catts, Grehn F, Hollo G, Khaw P, Overton B, Wilson R, et al. Factors affecting the outcome of trabeculectomy: an analysis based on combined data from two phase III studies of an antibody to transforming growth factor beta2, CAT-152. *Ophthalmol Times* 2007;**114**:1831–8.
16. Xu J, Khan AR, Fu M, Wang R, Ji J, Zhai G. Cell-penetrating peptide: a means of breaking through the physiological barriers of different tissues and organs. *J Contr Release* 2019;**309**:106–24.
17. Liu C, Tai L, Zhang W, Wei G, Pan W, Lu W. Penetratin, a potentially powerful absorption enhancer for noninvasive intraocular drug delivery. *Mol Pharm* 2014;**11**:1218–27.
18. Sakaguchi H, Takai S, Sakaguchi M, Sugiyama T, Ishihara T, Yao Y, et al. Chymase and angiotensin converting enzyme activities in a hamster model of glaucoma filtering surgery. *Curr Eye Res* 2002;**24**:325–31.
19. Pierce GF, Mustoe TA, Lingelbach J, Masakowski VR, Griffin GL, Senior RM, et al. Platelet-derived growth factor and transforming growth factor-beta enhance tissue repair activities by unique mechanisms. *J Cell Biol* 1989;**109**:429–40.
20. Cantor LB, Mantravadi A, WuDunn D, Swamynathan K, Cortes A. Morphologic classification of filtering blebs after glaucoma filtration surgery: the Indiana bleb appearance grading scale. *J Glaucoma* 2003;**12**:266–71.
21. Chang L, Crowston JG, Cordeiro MF, Akbar AN, Khaw PT. The role of the immune system in conjunctival wound healing after glaucoma surgery. *Surv Ophthalmol* 2000;**45**:49–68.
22. Wynn TA, Ramalingam TR. Mechanisms of fibrosis: therapeutic translation for fibrotic disease. *Nat Med* 2012;**18**:1028–40.
23. Honjo M, Tanihara H, Kameda T, Kawaji T, Yoshimura N, Araie M. Potential role of Rho-associated protein kinase inhibitor Y-27632 in glaucoma filtration surgery. *Invest Ophthalmol Vis Sci* 2007;**48**:5549–57.
24. Chen Z, Zhong C. Decoding Alzheimer's disease from perturbed cerebral glucose metabolism: implications for diagnostic and therapeutic strategies. *Prog Neurobiol* 2013;**108**:21–43.
25. Shah CA, Wang H, Bei L, Platanias LC, Eklund EA. HoxA10 regulates transcription of the gene encoding transforming growth factor beta2 (TGFbeta2) in myeloid cells. *J Biol Chem* 2011;**286**:3161–76.
26. Buczkowski A, Olesinski T, Zbicinska E, Urbaniak P, Palecz B. Spectroscopic and calorimetric studies of formation of the supramolecular complexes of PAMAM G5–NH_2 and G5–OH dendrimers with 5-fluorouracil in aqueous solution. *Int J Pharm* 2015;**490**:102–11.
27. Rothbard JB, Jessop TC, Wender PA. Adaptive translocation: the role of hydrogen bonding and membrane potential in the uptake of guanidinium-rich transporters into cells. *Adv Drug Deliv Rev* 2005;**57**:495–504.
28. Zhong L, Xu L, Liu Y, Li Q, Zhao D, Li Z, et al. Transformative hyaluronic acid-based active targeting supramolecular nanoplatform improves long circulation and enhances cellular uptake in cancer therapy. *Acta Pharm Sin B* 2019;**9**:397–409.
29. Calles JA, Tartara LI, Lopez-Garcia A, Diebold Y, Palma SD, Valles EM. Novel bioadhesive hyaluronan-itaconic acid crosslinked films for ocular therapy. *Int J Pharm* 2013;**455**:48–56.
30. Ito G, Kobayashi T, Takeda Y, Sokabe M. Proteoglycan from salmon nasal cartridge [corrected] promotes *in vitro* wound healing of fibroblast monolayers *via* the CD44 receptor. *Biochem Biophys Res Commun* 2015;**456**:792–8.

31. Jiang K, Gao X, Shen Q, Zhan C, Zhang Y, Xie C, et al. Discerning the composition of penetratin for safe penetration from cornea to retina. *Acta Biomater* 2017;**63**:123−34.
32. Ouyang D, Zhang H, Parekh HS, Smith SC. The effect of pH on PAMAM dendrimer−siRNA complexation: endosomal considerations as determined by molecular dynamics simulation. *Biophys Chem* 2011;**158**:126−33.
33. Lindberg S, Munoz-Alarcon A, Helmfors H, Mosqueira D, Gyllborg D, Tudoran O, et al. PepFect15, a novel endosomolytic cell-penetrating peptide for oligonucleotide delivery *via* scavenger receptors. *Int J Pharm* 2013;**441**:242−7.
34. Ramsey JD, Flynn NH. Cell-penetrating peptides transport therapeutics into cells. *Pharmacol Ther* 2015;**154**:78−86.
35. Tunnemann G, Martin RM, Haupt S, Patsch C, Edenhofer F, Cardoso MC. Cargo-dependent mode of uptake and bioavailability of TAT-containing proteins and peptides in living cells. *FASEB J* 2006;**20**:1775−84.
36. Pescina S, Ostacolo C, Gomez-Monterrey IM, Sala M, Bertamino A, Sonvico F, et al. Cell penetrating peptides in ocular drug delivery: state of the art. *J Contr Release* 2018;**284**:84−102.
37. David AL. Latent-TGF-β: an overview. *Mol Cell Biochem* 2001;**219**:163−70.